Solvated Electrons! The Missing Link in Highly Reducing Photocatalysis

Aslam C. Shaikh,[a†] Md Mubarak Hossain,[a†] Jules Moutet,[a] Anshu Kumar,[b] Benjamin Thompson,[c] Vanessa M. Huxter,[a,b] and Thomas L. Gianetti [a]*

[a]Department of Chemistry and Biochemistry, University of Arizona, Tucson, AZ 85721, United States.

[b]Department of Physics, University of Arizona, Tucson, AZ 85721, United States.

[c]Department of Optical Sciences, University of Arizona, Tucson, AZ 85721, United States.

[†]These authors contributed equally to this work

*Correspondence to: tgianetti@arizona.edu

Abstract

In recent years, in-situ generated organic radicals have been used as highly potent photoinduced electron transfer (PET) agents resulting in catalytic systems as reducing as alkaline metals that can activate remarkably stable bonds. However, the transient nature of these doublet state open-shell species has led to debatable mechanistic studies, hindering adoption and development. Herein, we document the use of an isolated and stable neutral organic radical as a highly photoreducing species with a reduction potential lower than – 3.5 V vs SCE. The isolated radical offers a unique platform to investigate the mechanism behind the photocatalytic activity of organic radicals. Our mechanistic study supports the involvement of solvated electrons formed by single electron transfer (SET) between the short-lived excited state organic radical and the solvent.

Introduction

Over the past decade, photoredox catalysis has received a fast and growing interest from the world of synthetic chemistry.[1,2] By combining visible light with a photocatalyst (PC), a large variety of efficient and selective transformations have been achieved under mild conditions, during which the excited state PC* is

involved in a single electron transfer (SET) with a substrate or a co-catalyst.[3,4] However, SET with a conventional photocatalyst is usually limited to redox potentials between - 2.0 V and + 2.0 V vs. Saturated Calomel electrode (SCE) (**Figure 1A**).[1,5] In recent years, several elegant reports have shown that open-shell doublet organic radicals, generated in-situ, either electrochemically[6,7] or photochemically via a consecutive two-photon excitation process,[8] can act as potent photoreducing agents.[9] In both processes, the open-shell doublet organic radical $PC^{\bullet}$ (anionic or neutral) is generated in-situ from a closed-shell singlet species (neutral or cationic), followed by photoexcitation generating the radical excited state $PC^{\bullet *}$ that can act as a super photoreducing agent ($E_{1/2}^{red*}$ = -2.3 to -3.4 V vs SCE).[10] The concept of a two-photon excitation process, commonly purported as a consecutive photoelectron transfer (conPET) pathway, has been reported with numerous notable photocatalysts such as PDI, DCA, anthraquinone, Rhodamine 6G, benzo[*ghi*]perylene (BPI), 4-DPAIPN, 3-CzEPAIPN, Mes-Acr, and Deazaflavin.[11-19] As a common benchmark reaction, photoredox C(sp^2)-X bond activation in aryl bromides and chlorides, Birch reduction, and sulfonamide cleavage has showcased the extreme photoreducing ability of radical photocatalysts. Despite convincing reports, an intriguing aspect of the photoactivity of open-shell doublet organic radicals is the short lifetime of their excited state (fs to ps), which should hamper their participation in bimolecular reactions with substrates.[20] Instead, closed-shell singlet species, such as a Meisenheimer complex or side product impurities, formed *in-situ* from the reactive open-shell doublet radicals have been reported as potential long-lived super-reducing photoreagents. However, the photophysical properties of these side products cannot explain the activation of substrates with reduction potentials lower than -2.8 V vs SCE. The transient nature of most organic radicals used to date hinders the full understanding of their mechanism (**Figure 1B**). Therefore, the synthesis and isolation of photoactive organic radicals are of great interest in order to shed light on the ability of open-shell doublet species to act as super photoreducing agents.

We recently reported the use of *N,N′*-di-*n*-propyl-1,13-dimethoxyquinacridinium (^{n}Pr-$DMQA^{+}$) tetrafluoroborate[21-22] as an organic photoredox catalyst for photoreductions and photooxidations under red light excitation (λ_{max} = 640 nm).[23-24] In our contemporary studies, we reported the chemical synthesis,

isolation, and characterization of the neutral helicene radical analog *N,N′*-di-*n*-propyl-1,13-dimethoxyquinacridine (^{n}Pr-DMQA$^{\bullet}$) as part of a family of neutral quinolinoacridine radicals.[25-26] Our studies show that this radical can be made on a gram scale, is highly persistent in its solid form as well as in solution for several months under inert conditions, and reversibly oxidizes back to the cation upon exposure to air. Herein, we report the use of the isolated ^{n}Pr-DMQA$^{\bullet}$ radical as a unique platform to investigate the mechanism of a highly reducing organic radical photocatalyst (**Figure 1C**). Our mechanistic study has revealed that the stable neutral helicene radical has a reduction potential lower than – 3.5 V vs SCE, and can photochemically generate solvated electrons by reducing acetonitrile or benzene. Hydrated electrons have enjoyed a renewed interest and have been posited as super-reducing intermediates during photocatalytic reduction in aqueous media[27,28] or alcohols.[15] However, an experimental system able to provide conclusive evidence that solvated electrons, especially in non-protic organic solvents, are key intermediates in potent photoreductive transformations remains elusive. Importantly, proving the involvement of solvated electrons in highly reducing photocatalytic systems reconciles the potential disconnect between the photocatalytic activity observed by several groups and the short-lived excited states of organic radical photocatalysts.

Results and Discussion

Photochemical and photocatalytic activity of ^{n}PrDMQA$^{\bullet}$ radical. The stable doublet organic neutral radical ^{n}Pr-DMQA$^{\bullet}$ was synthesized by the chemical reduction of ^{n}Pr-DMQA^{+} using CoCp*$_2$. This radical was found to possess strong absorption of light in the visible region (391 nm, 440 nm, 467 nm, and 557 nm) and a weaker absorbance centred around 650 nm (Figure 1C). To probe the photoreducing ability of the ^{n}Pr-DMQA scaffold, we first monitored by UV-Vis spectroscopy the irradiation of a solution containing ^{n}Pr-DMQA$^{\bullet}$ and excess of 4-bromo anisole ($E_{1/2}^{red}$ = - 2.90 V vs SCE) with a 440 nm and a 640 nm LED (Supplementary Figure S2 – S3). Under 640 nm irradiation or in absence of light no change to the UV-Vis spectra were observed. However, under 440 nm irradiation, we observed the disappearance of the radical

^{n}Pr-DMQA$^{\bullet}$ absorption band and the appearance of the cation ^{n}Pr-DMQA^{+} absorption bands (**Figure 2A**). We then performed a stoichiometric photo-Arbuzov reaction, with triethyl phosphite $P(OEt)_3$ as radical trapping agent, using different light sources (440 nm and 640 nm), different DMQA species (^{n}Pr-DMQA$^{\bullet}$, ^{n}Pr-DMQA^{+}), and different aryl bromide substrates with a range of reduction potentials (4-bromo benzonitrile 2a, $E_{1/2}^{red}$ = -1.94 V vs SCE; and 4-bromo anisole 2b, $E_{1/2}^{red}$ = -2.90 V vs SCE) (**Figure 2B**, and Supplementary Table S1). Using ^{n}Pr-DMQA^{+}, under either 440 nm or 640 nm irradiation, did not produce any aryl-activated product consistent with the mild photoreducing potential of the closed shell singlet cation species (Supplementary Table S1). On the other hand, when the open-shell doublet neutral radical ^{n}Pr-DMQA$^{\bullet}$ was irradiated under 440 nm both aryl halides were activated, with a higher yield for the less electron-rich bromo benzonitrile (3a, <90% yield) and 3b, 50% yield, **Figure 2B**).

Consistent with our previous observations,[23,25] EPR experiments as well as UV-Vis spectroscopy, revealed that ^{n}Pr-DMQA$^{\bullet}$ can be generated in-situ by irradiating ^{n}Pr-DMQA^{+} with either 440 nm blue or 640 nm red-light sources in presence of three different electron donors (**Figure 2C,** and Figure S4 – S7). Inspired by the stoichiometric photo-Arbuzov experiment and the photochemical generation of ^{n}Pr-DMQA$^{\bullet}$ from ^{n}Pr-DMQA^{+}, we attempted the catalytic reductive dehalogenation of 4-bromo benzonitrile ($E_{1/2}$ = -1.94 V and BDE = 80 kcal/mol)[29] and 4-bromo anisole ($E_{1/2}$ = -2.90 V and BDE > 85 kcal/mol) in presence of pyrrolidine with ^{n}Pr-DMQA^{+} or ^{n}Pr-DMQA$^{\bullet}$ as a photocatalyst under either blue (440 nm) or red (640. nm) light (**Figure 2D,** and Supplementary Table S1). In the case of 4-bromo anisole, both PCs induced a dehalogenation reaction under blue light with similar yields. However, no product was detected with either PC when 640 nm light was employed, consistent with the fact that ^{n}Pr-DMQA$^{\bullet}$ has little absorption at that wavelength, and that ^{n}Pr-DMQA^{+*} is not reductive enough to undergo PET with aryl halides. Similarly, with the electron-poor bromo benzonitrile, both PCs afforded full conversion under blue light (**Figure 2D**). However, unlike with anisole, some conversions were detected with both ^{n}Pr-DMQA^{+} and ^{n}Pr-DMQA$^{\bullet}$ under 640 nm light. Recent reports have shown that a photochemically generated ammonium radical can initiate a XAT mechanism with electron-poor substrates such as 4-bromobenzonitrile.[30,31] Together, these

observations suggest that easily reducible substrates ($E_{1/2}^{red}$ > - 2.0 V vs SCE) such as 4-bromobenzonitrile can be activated by the ^{n}Pr-DMQA platform via either SET or XAT mechanisms. However, for electron-rich species such as 4-bromo anisole, blue light and ^{n}Pr-DMQA$^{\bullet}$ are required, suggesting that PET from ^{n}Pr-DMQA$^{\bullet}$ is a suitable pathway.

The scope of catalytic reductive dehalogenation of aryl halides was performed as the benchmark reaction to evaluate the extent of the reducing potency of ^{n}Pr-DMQA$^{\bullet}$. Under optimal reaction conditions (Supplementary Table S2) in either acetonitrile or toluene, successful dehalogenation of a variety of electron-rich aryl bromides and chlorides, have been demonstrated in good to excellent yields (**4a**-**4r**, 81-99 % yield, see **Table 1a**, and ESI), including substrates with reduction potentials lower than -3.50 V vs SCE (See ESI, $E_{1/2}$ (**4f**) < - 3.5 V vs SCE, $E_{1/2}$ (**4g**) = - 3.1 V vs SCE,). Polyaromatic substrates and heteroaromatic bromides were also found to be efficient substrates for reductive dehalogenation (**4s-4t**, 80-96 % yield). In general, aryl halides bearing nitrile (4c), ester (4d, 4n), trifluoromethyl (4e, 4s), ketone (4m), free acid (4p), free hydroxy (4q) and free amine (4r) groups were well-tolerated and found to be excellent substrates for this neutral helicene radical catalyzed photoredox dehalogenation. Catalytic functionalization of these substrates were extended to C-P bond formation via photo-phosphorylation, C-B bond formation via photo-borylation, and C-C bond formation via a-arylation of pyrroles and cyclic ketones (See **Table 1b**, and ESI for more details and discussions). These transformations show the versatility of the system in the synthesis of valuable chemicals such as aryl borate, important coupling partner in late-stage derivatization, and aryl phosphonates, critical building blocks for numerous pharmaceutical agents and bioactive natural products.[32]

Mechanistic evidence of solvated electrons: Previous reports have shown that the neutral species ^{n}Pr-DMQA-H can be formed during the electrochemical reduction of ^{n}Pr-DMQA$^{\bullet}$ to ^{n}Pr-DMQA^{-}, or by reaction between an hydride donor and ^{n}Pr-DMQA^{+} (See ESI).[33] Considering the recent reports suggesting that *in-situ* generated closed-shell singlet side products can be involved during photochemical transformations,[20] we first turned our focus on ^{n}Pr-DMQA-H. Following the Lacour *et. al*. synthetic protocol,[33] we have

synthesized and studied the electro- and photophysical properties of this neutral closed-shell singlet (see ESI). The UV-Vis spectroscopy of ^{n}Pr-DMQA-H shows the presence of a photo-inactive species that possesses an absorption at 316 nm (Supplementary Figure S9). The cyclic voltammogram of ^{n}Pr-DMQA-H (**Figure 3A**, and Supplementary Figure S14) reveals an irreversible oxidation event at +0.67 V vs SCE, followed by a reversible oxidation at + 1.27 V vs SCE which was assigned to the ^{n}Pr-DMQA$^{++\bullet}$ / ^{n}Pr - DMQA^{+} redox couple, suggesting that ^{n}Pr-DMQA^{+} is electrochemically generated from the oxidation of ^{n}Pr-DMQA-H.[34] Interestingly, ^{n}Pr-DMQA-H, which can be formed by irradiation of ^{n}Pr-DMQA$^{\bullet}$ at 440 nm in presence of amine (Supplementary Figure S9), was found to be stable in acetonitrile in the absence of oxygen and in the dark, but undergoes photoinduced homolysis to form ^{n}Pr-DMQA$^{\bullet}$ when irradiated with a 440 nm LED (**Figure 3A**, and Supplementary Figure S11). These results support that the closed shell singlet ^{n}Pr-DMQA-H is expected to form under photocatalytic condition as an off-cycle intermediate which converts back to ^{n}Pr-DMQA$^{\bullet}$ via photolysis, or to ^{n}Pr-DMQA^{+} under mild oxidative conditions, undermining its involvement as a possible potent photoinduced electron transferring agent responsible for the reduction of electron-rich aryl halides.

To further understand the photocatalytic mechanism involved with the present system, we then considered the photophysical properties of the open-shell doublet neutral radical ^{n}Pr-DMQA$^{\bullet}$. We observed that despite its strong absorption in the visible region, ^{n}Pr-DMQA$^{\bullet}$ generated by reduction of ^{n}Pr-DMQA^{+} with cobaltocene was found to be non-emissive (**Figure 3Bi**, Supplementary Figure S18) and its excited state lifetime to be sub-nanosecond (*vide-infra*). This is unsurprising as radicals in solution are generally non-emissive due to competing non-radiative decay pathways and short lifetimes.[35,36] We then monitored the UV-Vis spectroscopy of ^{n}Pr-DMQA$^{\bullet}$ under irradiation at 440 nm. In acetonitrile alone, no clear change was observed in the absorption spectra (Supplementary Figure S16), but a growing signal at 593 nm (**Figure 3Bii**, and Supplementary Figure S17) was observed in the fluorescence emission spectra along with the formation of ^{n}Pr-DMQA^{+} (660 nm emission peak). However, no emission was detected when ^{n}Pr-DMQA$^{\bullet}$ was irradiated at 440 nm in benzene suggesting that ^{n}Pr-DMQA$^{\bullet}$ reacts with CH_3CN under 440 nm

irradiation. Importantly, formation of CDH_2CN and CHD_2CN was observed by ^1H NMR spectroscopy, when ^{n}Pr-DMQA$^\bullet$ was irradiated at 440 nm in a mixture of CH_3CN/CD_3CN (1:1 and 1:9 ratio) implying the generation of acetonitrile radical $^\bullet CH_2CN/^\bullet CD_2CN$ (**Figure 3C** and Supplementary Figure S23). Yet, no scrambling was observed when a mixture of THF/THF-d_8 was used, excluding the involvement of a direct H atom abstraction mechanism ($BDE_{C\text{-}H(THF)}$ = 85 kcal/mol and $BDE_{CH(CH3CN)}$ = 83 kcal/mol) (Supplementary Figure S25). Williams *et. al*. reported that gamma irradiated acetonitrile led to an electron solvation between two acetonitrile molecules ($[(CH_3CN)_2]^{\bullet-}$), which rapidly fragmentate to $^\bullet CH_3$ and CN^-, generating methane and $^\bullet CH_2CN$ (**Figure 3C** inset).[37,38] Fluorescence emission spectra of the thermal product formed between ^{n}Pr-DMQA$^\bullet$ and AIBN, a known $^\bullet C(CH_3)_2CN$ radical generator, revealed the formation of an emissive species at 590 nm (Supplementary Figure S26) . These observations, along with the ability for our system to reduce substrates with redox potentials lower than - 3.5 V vs. SCE (*vide supra*), suggests that the excited state ^{n}Pr-DMQA$^{\bullet *}$ generated under 440 nm irradiation undergoes PET with acetonitrile to form a solvated electron $[(CH_3CN)_2]^{\bullet-}$ ($E_{1/2}$ ($CH_3CN/CH_3CN^{-\bullet}$) = - 3.45 V vs SCE).[37,39] Fragmentation of $[(CH_3CN)_2]^{\bullet-}$ generates $^\bullet CH_2CN$, which can further react with the ^{n}Pr-DMQA scaffold to form an emissive species (*vide-supra* and ESI). Emission characteristic of ^{n}Pr-DMQA$^+$, along with an emissive species with a maxima at 590 nm, was detected when ^{n}Pr-DMQA$^\bullet$ was irradiated at 440 nm in presence of 4-bromo anisole or bromobenzene, in benzene (**Figure 3Biii,** and Supplementary Figure S19-21), consistent with the efficient stoichiometric photo Arbuzov and catalytic functionalization of aryl halide in both toluene and acetonitrile (*vide supra*). Since no emissive species was observed in benzene alone, and in light of the sub-nanosecond lifetime of ^{n}Pr-DMQA$^{\bullet *}$ (*vide supra* and ESI), these observations suggest that PET occurs between ^{n}Pr-DMQA$^\bullet$ and the solvent, generating a solvated electrons as longer-lived potent reducing species.

To further probe the ability of ^{n}Pr-DMQA$^\bullet$ to undergo photoinduced electron transfer with aryl halides via reduction of the solvent and solvated electrons, we performed transient absorption (TA) measurements using a home-built apparatus with broadband detection (see ESI for additional experimental details). For

all TA traces, samples were excited at 560 nm, resonant with the main absorption feature in the visible of the ^{n}Pr-DMQA• neutral radical (D_2 state). TA analysis of the ^{n}Pr-DMQA• neutral radical was performed in acetonitrile, deuterated acetonitrile, and benzene (**Figure 3Di-iii** and Supplementary Figure S29-32). In all traces, two positive signals are present on either side of the ground state bleach at 560 nm. The feature peaked at 587 nm is an excited state absorption, which appears at the same energy in all three solvents. The positive feature to the higher energy side of the ground state bleach has two contributions, an excited state absorption centred at 500 nm and a photoproduct at 524 nm. The feature centred at 500 nm also appears in the same place in all three solvents, while the photoproduct signal at 524 nm is present in acetonitrile and deuterated acetonitrile. The signal at 524 nm in acetonitrile and deuterated acetonitrile persists beyond the maximum delay of the experiment (1 ns). Stimulated emission signal from the photoproduct is not evident as it is likely overlapped with the ground state bleach or a strong excited state absorption signal. Plots of an integrated region of the TA measurement from 520 to 530 nm shows the persistence of the signal at 524 nm in acetonitrile and deuterated acetonitrile as well as the decay of the signal to baseline in benzene (**Figure Di**).

TA measurements of the ^{n}Pr-DMQA• neutral radical in acetonitrile in the presence of an aryl halide (4-bromo anisole) with a ratio of 1:1, 1:10 and 1:100 was performed (**Figure 3Div-vi** and Supplementary Figure S33-36). In these traces, the ^{n}Pr-DMQA• excited state absorption centred at 587 nm shifts to 616 nm, indicating the *in*-situ generation of the cation ^{n}Pr-DMQA^{+} cation photoproduct. Stimulated emission associated with the cation can also be observed at 665 nm. The photoproduct at 524 nm and the excited state absorption at 500 nm seen in acetonitrile alone are also observed. Integrated regions of the TA data for different ratios of aryl halide from 520 to 530 nm (**Figure Div**) and from 585 to 595 nm (Supplementary Figure S36) show little change in the TA signal, indicating that the reaction rate is not determined by the ratio of ^{n}Pr-DMQA• to aryl halide. This is consistent with the formation of a long-lived solvated electron[40,41] from the reduction of the acetonitrile solvent by the excited state ^{n}Pr-DMQA$^{•*}$ radical.

Taken together with the linear UV-Vis spectroscopy and scrambling experiments, these preliminary mechanistic data suggest that, under 440 nm irradiation, the excited state of ^{n}Pr-DMQA$^{\bullet}$ undergoes PET with the solvent. In absence of aryl halide, fast back electron transfer occurs in benzene ($E_{1/2}$ ($C_6H_6/C_6H_6^{-\bullet}$) = - 3.42 V vs SCE),[42] while in acetonitrile some formation of $^{\bullet}CH_2CN$ radical is detected due to the fragmentation of [$(CH_3CN)_2^{-\bullet}$]. In presence of aryl halide, the reduced solvent serves as a carrier of solvated electrons for the reduction of aryl halide leading to the formation of an aryl radical. Both Ar$^{\bullet}$ and $^{\bullet}CH_2CN$ can interact with the ^{n}Pr-DMQA scaffold, to form an emissive photoproduct similar to the neutral emissive species formed between the thermal decomposition of AIBN and ^{n}Pr-DMQA$^{\bullet}$.

Conclusion

In summary, while several reports have supported the involvement of open-shell doublet radicals as potent photoreducing species, the isolation of a stable photoactive radical that can allow an extensive mechanistic study has remained elusive. Herein, we have reported that the stable and isolable open-shell doublet radical *N,N'*-di-*n*-propyl-1,13-dimethoxyquinacridine (^{n}Pr-DMQA$^{\bullet}$) is a highly reducing photocatalyst. We first probed the photoreducing ability of the ^{n}Pr-DMQA$^{\bullet}$ using a stoichiometric photo-Arbuzov reaction with an electron-poor (4-bromo benzonitrile) and an electron-rich (4-bromo anisole) aryl bromide, under both 440 and 640 nm excitation. The results obtained, coupled to the control experiments using ^{n}Pr-DMQA^{+}, substantiate that the helicene radical is a potent photoinduced electron transferring agent under 440 nm irradiation. Our preliminary mechanistic study, involving UV-Vis spectroscopy, deuterium scrambling experiments and transient absorption spectroscopy in CH_3CN, CD_3CN and benzene as well as with an increasing amount of aryl halide, revealed that the non-emissive short-lived excited state ^{n}Pr-DMQA$^{\bullet *}$ undergoes PET with the solvent resulting in solvated electrons as key intermediates in the reduction of electron-rich aryl halides. The involvement of solvated electrons renders the requirement for a long-excited lifetime of the photocatalyst obsolete. We are currently continuing to investigate the mechanism of this transformation and the use of the ^{n}Pr-DMQA platform as alternative way for streamline the synthesis of complex functionality in both academia and industry.

Methods

ⁿPrDMQA radical synthesis: Inside a N2 filled glovebox, to a dark blue-green suspension of **ⁿPrDMQA**$^+$ (350mg, 0.70 mmol, 1 eq.) in THF, 1 equivalent of bis(pentamethylcyclopentadienyl)cobalt ($CoCp^*_2$, 235mg, 0.71 mmol, 1 eq.) was added at room temperature under vigorous stirring. The mixture slowly turned deep red from the initial dark green colour overnight. After filtration of the insoluble $(CoCp^*_2)BF_4$ salt through a PTFE milliport filter syringe, THF was removed under vacuum to afford a dark red residue. This resultant solid was triturated in a mixture of toluene and hexane before solvents removal. The shiny residue was then extracted with toluene and concentrated under vacuum. Concentrated solution of toluene mixtures was layered with hexane at -35°C to afford **ⁿPrDMQA** radical as dark blood-red crystals.

General procedure for hydro-dehalogenation reaction: In nitrogen-filled glove box, an oven dried 10 mL Schlenk tube equipped with magnetic stir bar was charged with ⁿPr-DMQA-BF_4 (2.5 mg, 5 mol%) and aryl halide substrate (0.10 mmol, 1.0 equiv., if solid). The solid mixture was dissolved in 0.5 ml (0.2 M) degassed solvent (acetonitrile), then aryl halide substrate (**4**, 0.10 mmol, 1.0 equiv., if liquid) and pyrrolidine (25 ul, 0.30 mmol, 3.0 equiv.) was added via syringe or micropipette. Then the Schlenk tube was removed from the glove box and placed in a water bath approximately 5 cm away from a Kessil 440 nm blue LED lamp. The reactions were stirred for 16 hours under irradiation with 440 nm LEDs. After completion, the reaction mixture was dissolved with $CDCl_3$ followed by addition of trimethoxy benzene (16.8 mg, 0.10 mmol, 1.0 equiv.) as the internal standard, and the yield of the desired product was determined via proton NMR spectroscopy.

In case of 4z substrate (1,3-dichloro-5-methoxybenzene), 0.5 M reaction concentration and two LED lamp were employed. The crude NMRs for determination of yield with internal standards are given in the NMR spectral data section.

General Procedure for Phosphodehalogenation reaction: In nitrogen-filled glove box, an oven dried 10 mL Schlenk tube equipped with magnetic stir bar was charged with ^{n}Pr-DMQA-BF_4 (**1**) (2.5 mg, 0.005 mmol, 0.050 equiv.) and aryl halide substrate (0.10 mmol, 1.0 eqiuv., if solid). The solid mixture was dissolved in 1 ml (0.1 M) degassed solvent (acetonitrile), then triethylphosphite (52 µl, 0.30 mmol, 3.0 equiv.), aryl halide substrate (0.10 mmol, 1.0 equiv., if liquid) and DIPEA (52 µl, 0.30 mmol, 3.0 equiv.) was added via syringe or micropipette. Then the Schlenk tube was removed from the glove box and placed in a water bath approximately 5 cm away from a Kessil 440 nm blue LED lamp. The reactions were stirred for 16 hours under irradiation with 440 nm LEDs. After completion, the reaction mixture was concentrated in vacuo then the yield was detected by two methods: 1) the desired product was isolated by flash column chromatography; 2) the reaction mixture was dissolved with $CDCl_3$ followed with addition of trimethoxy benzene (16.8 mg, 0.10 mmol, 1.0 equiv.) as the internal standard, and the yield of the desired product was determined via proton NMR spectroscopy.

General procedure for boro-dehalogenation reaction: In nitrogen-filled glove box, an oven dried 10 mL Schlenk tube equipped with magnetic stir bar was charged with ^{n}Pr-DMQA-BF_4 (**1**) (2.5 mg, 0.005 mmol, 0.050 equiv.) and aryl halide substrate (0.10 mmol, 1.0 equiv., if solid). The solid mixture was dissolved with 1 ml (0.1 M) degassed solvent (acetonitrile), then bis(pinacolato)diboron (75 mg, 0.30 mmol, 3.0 equiv.), aryl halide substrate (0.10 mmol, 1.0 eq, if liquid) and DIPEA (52 µl, 0.30 mmol, 3.0 equiv.) was added via syringe or micropipette. Then the Schlenk tube was removed from the glove box and placed in a water bath approximately 5 cm away from a Kessil 440 nm blue LED lamp. The reactions were stirred for 16 hours under irradiation with 440 nm LEDs. After completion, the reaction mixture was concentrated in vacuo then the yield was detected by two methods: 1) the desired product was isolated by flash column chromatography; 2) the reaction mixture was dissolved with $CDCl_3$ followed by addition of trimethoxy benzene (16.8 mg, 0.10 mmol, 1.0 eq) as the internal standard, and the yield of the desired product was determined via proton NMR spectoscopy.

General Procedure for carbo dehalogenation reaction: In nitrogen-filled glove box, an oven dried 10 mL Schlenk tube equipped with magnetic stir bar was charged with ^{n}Pr-DMQA-BF_4 (**00**) (2.5 mg, 0.005 mmol, 0.050 equiv.) and aryl halide substrate (0.10 mmol, 1.0 equiv., if solid). The solid mixture was dissolved with 1 ml (0.1 M) degassed solvent (acetonitrile), then *N*-methyl pyrrole (28 µl, 0.30 mmol, 3.0 equiv., aryl halide substrate (0.10 mmol, 1.0 equiv., if liquid) and DIPEA (52 µl, 0.30 mmol, 3.0 equiv.) was added via syringe or micropipette. Then the Schlenk tube was removed from the glove box and placed in a water bath approximately 5 cm away from a Kessil 440 nm blue LED lamp. The reactions were stirred for 16 hours under irradiation with 440 nm LEDs. After completion, the reaction mixture was concentrated in vacuo then the yield was detected by two methods: 1) the desired product was isolated by flash column chromatography; 2) the reaction mixture was dissolved with $CDCl_3$ followed by addition of trimethoxy benzene (16.8 mg, 0.10 mmol, 1.0 equiv.) as the internal standard, and the yield of the desired product was determined via proton NMR spectroscopy.

ACKNOWLEDGMENTS

We thank Dr. Jixun Dai and Dr. Andrei Astashkin for their help in performing NMR and EPR measurements.

Fundings: T.L.G and V.M.H gratefully acknowledge support from the University of Arizona. This research was supported by the National Science Foundation through CAREER award grant no. 2144018 (T.L.G.) and grant no. 1920234 (University of Arizona), as well as the American Chemical Society Petroleum Research Fund through grant no. 65536-ND6 (V.M.H.).

Author contributions: T.L.G. supervised the project. A.C.S. and M.M.H. performed the stoichiometric and catalytic transformations. A.C.S., M.M.H., A.K and B.T. recorded absorption and emission spectra. J.M.M. synthesized the DMQA radical and performed the cyclic voltametric experiments, M.M.H. performed deuterium scrambling experiments. V.M.H. supervised and designed the time-resolved and linear spectroscopy experiments, A.K and B.T. collected the time-resolved spectra. T.L.G., A.C.S., M.M.H. and V.M.H. wrote the paper. All authors participated in active discussions and reviewed the manuscript.

Competing interests: Authors declare that they have no competing interests.

Data and material availability: All data are presented in supplementary materials.

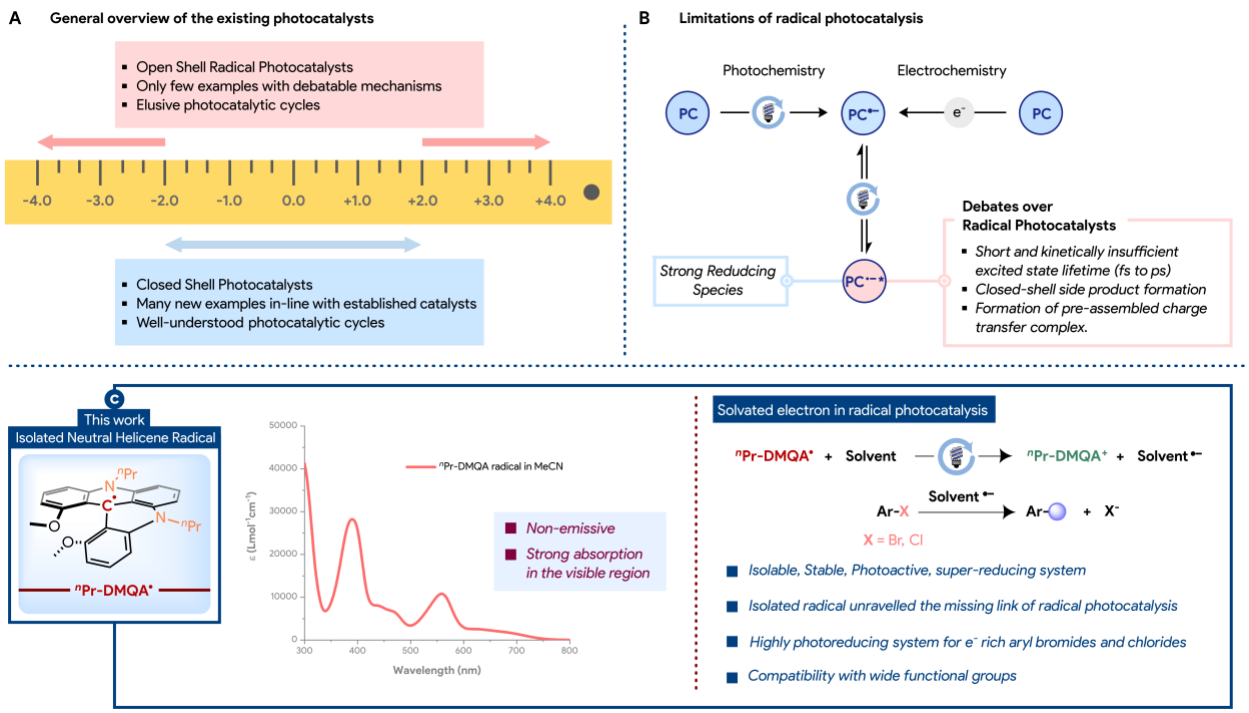

Figure 1: A. General overview of the current state of the art for photocatalysis, highlighting the scarcity of systems able to perform photoredox chemistry outside the -2.0V to +2.0V vs SCE window; **B.** *In-situ* photochemical or electrochemical generation of the organic radical photocatalyst incurs an ambiguous and inefficient photocatalytic mechanism; **C.** This work, using an isolated ^{n}Pr-DMQA radical as a potent photoreducing system, and a unique platform for the mechanistic investigation of an open-shell doublet organic photocatalyst supporting the involvement of solvated electrons. PC, photocatalyst.

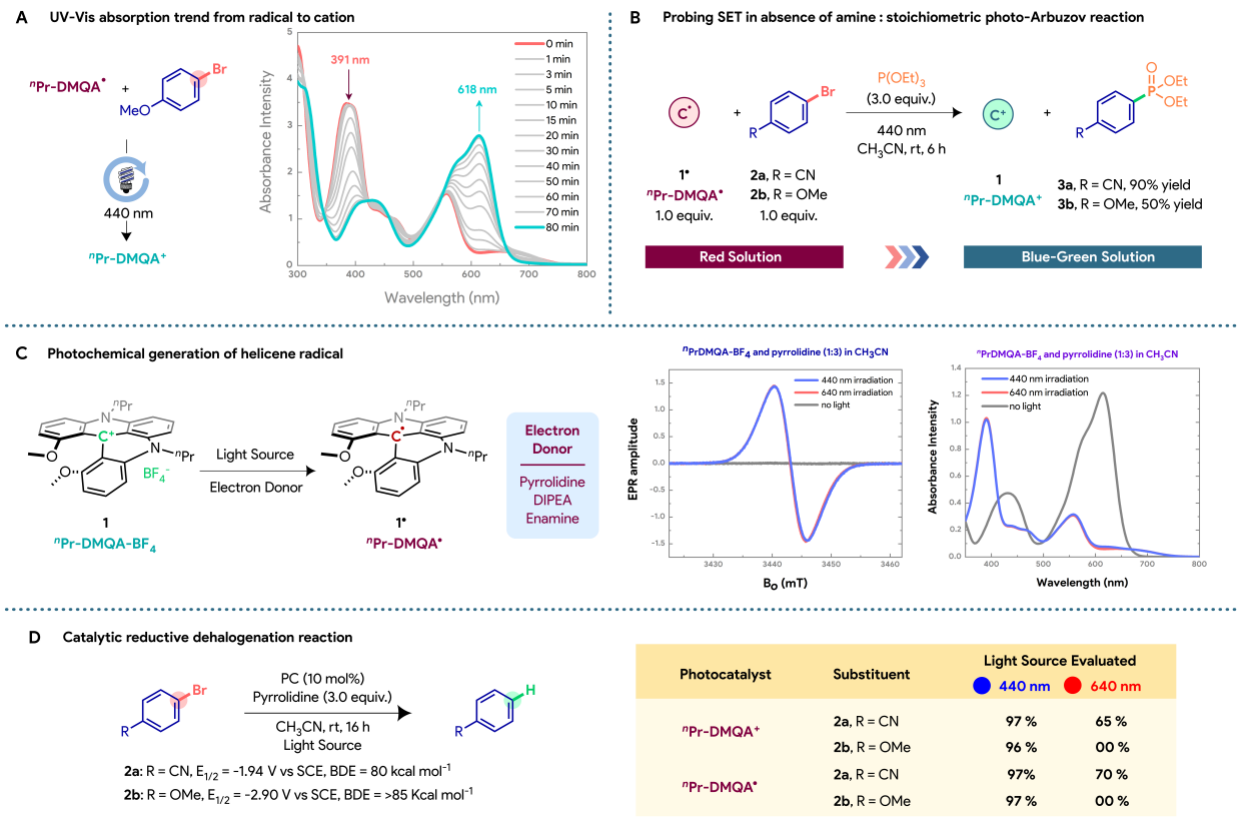

Photocatalyst	Substituent	Light Source Evaluated: 440 nm	640 nm
nPr-DMQA+	2a, R = CN	97 %	65 %
	2b, R = OMe	96 %	00 %
nPr-DMQA•	2a, R = CN	97%	70 %
	2b, R = OMe	97 %	00 %

Figure 2: A. UV-visible spectroscopic monitoring of the reaction between ^{n}Pr-DMQA$^{\bullet}$ and 4-bromo anisole in acetonitrile under 440 nm irradiation, resulting in the formation of ^{n}Pr-DMQA^{+}; **B.** Stoichiometric photo-Arbuzov reaction to evaluate direct SET pathway and proof of concept for the photoreducing ability of the isolated ^{n}Pr-DMQA$^{\bullet}$; **C**. Photochemical generation of ^{n}Pr-DMQA$^{\bullet}$ and detection by EPR and UV – Vis spectroscopy; **D.** Catalytic reductive dehalogenation reaction of aryl bromides using ^{n}Pr-DMQA^{+} and ^{n}Pr-DMQA$^{\bullet}$ under 440 nm and 640 nm irradiation.

Table 1: Substrate scope for photocatalytic dehalogenation and functionalization of electron rich aryl halides. [a] 0.5 M reaction concentration and 24 h reaction time. [b] 0.5 M reaction concentration and two LED lamps were used. See the supporting information for more reaction details.

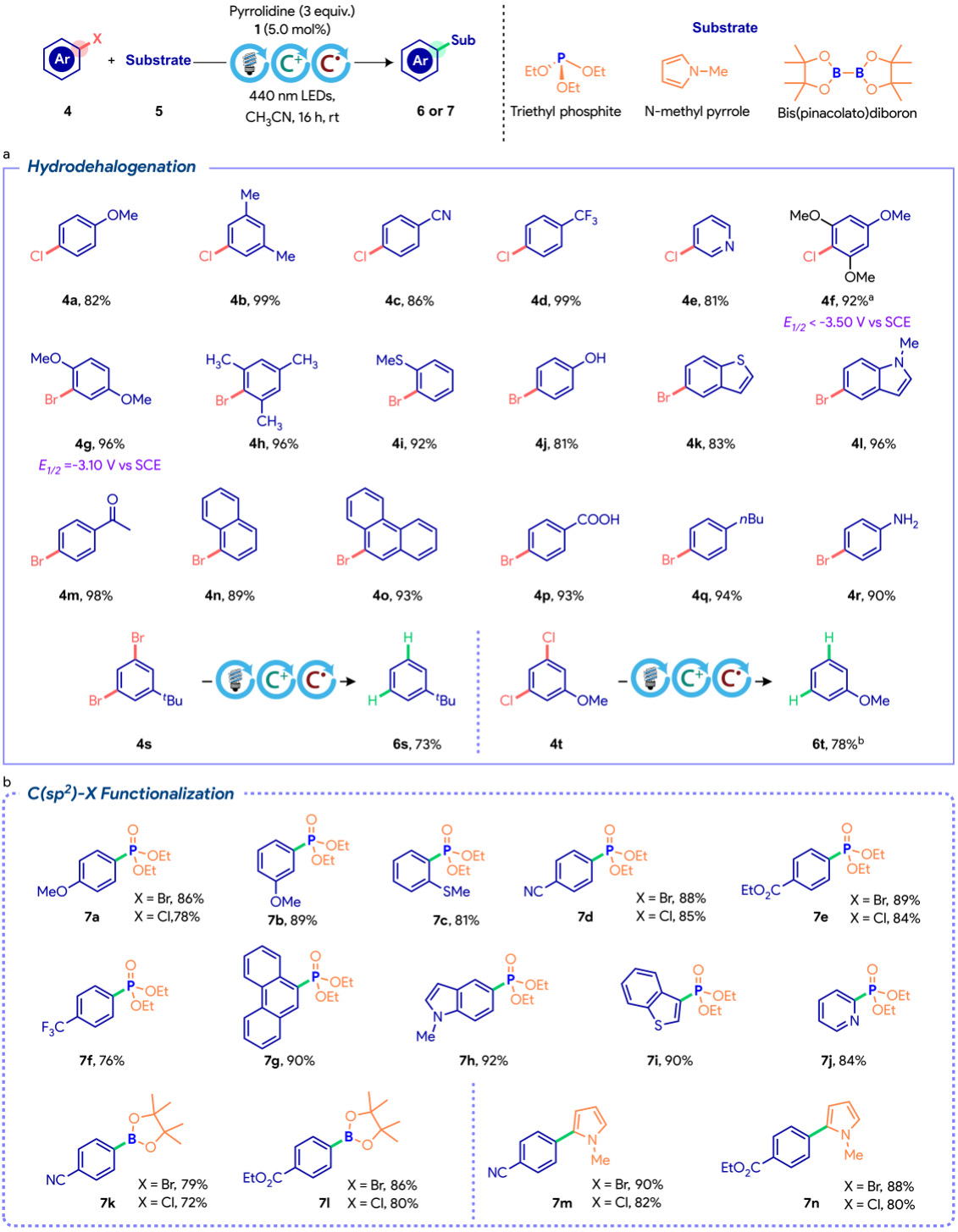

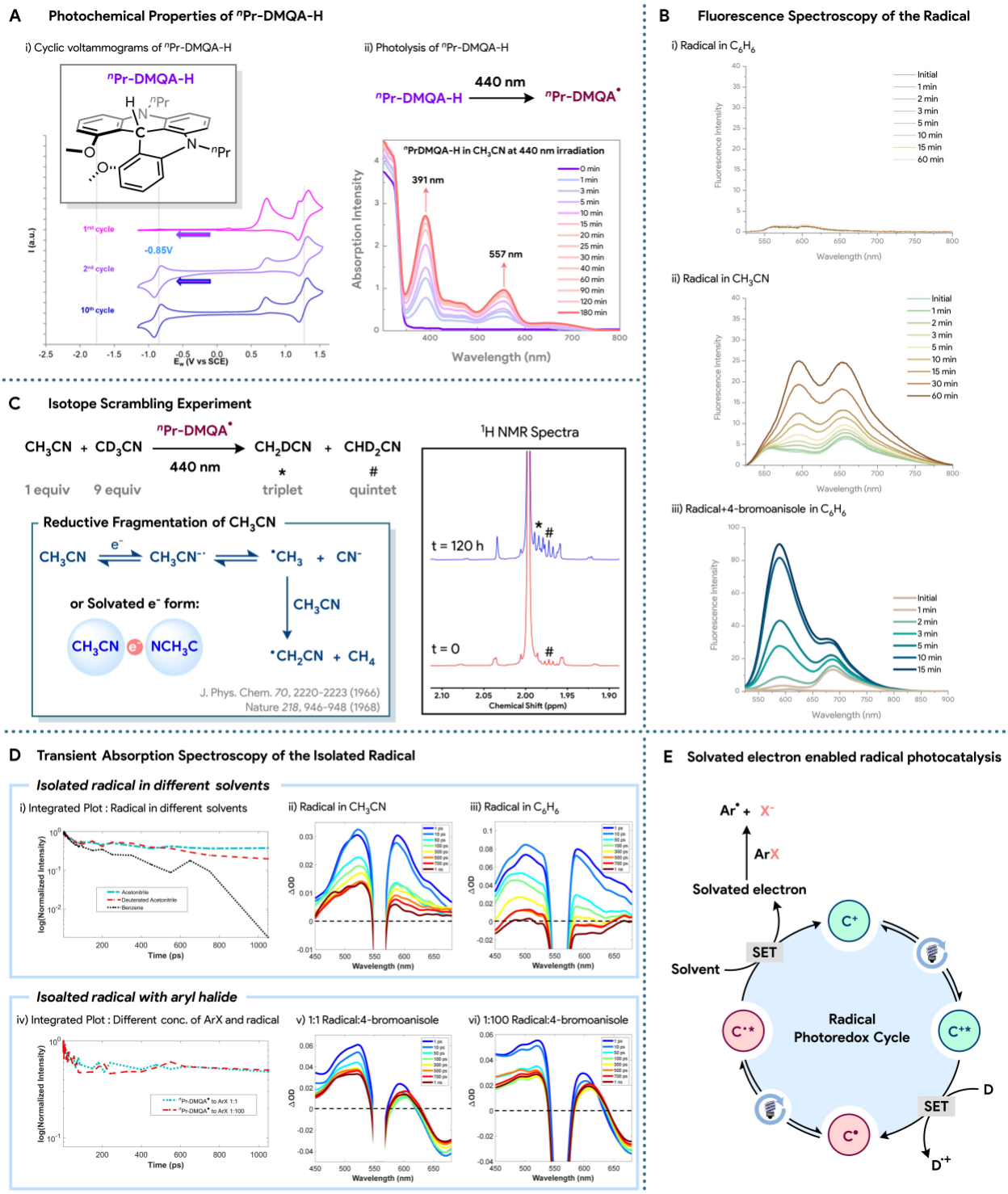

Figure 3: A. Electrochemical and photophysical behavior of the nPr-DMQA-H species, (**i**) Cyclic voltammetry of ^{n}Pr-DMQA-H species, (**ii**) Photolysis of ^{n}Pr-DMQA-H into ^{n}Pr-DMQA radical under 440 nm light irradiation, **B.** Fluorescence spectrum of ^{n}Pr-DMQA$^{\bullet}$ in Benzene showing no emission (**i**), in

CH_3CN alone (**ii**) and in benzene with 4-bromo anisole (**iii**) showing emission around 590 nm and the cationic ^{n}Pr-DMQA^{+} emission between 650 and 700 nm. **C**. Isotope scrambling experiments from the irradiation of ^{n}Pr-DMQA$^{\bullet}$ at 440 nm in a mixture of CH_3CN and CD_3CN showing the formation of CH_2DCN and CHD_2CN in ^{1}H NMR spectroscopy. **D.** Photophysical studies of the ^{n}Pr-DMQA$^{\bullet}$ neutral radical in absence of aryl halide. (**i**) Integrated TA signal for ^{n}Pr-DMQA$^{\bullet}$ in acetonitrile, deuterated acetonitrile, and benzene for the 520-530 nm region associated with the photoproduct presented on a semi-log scale, (**ii**) TA frequency-resolved slices at selected time delays for ^{n}Pr-DMQA$^{\bullet}$ in acetonitrile, and (**iii**) in benzene.; Photophysical studies of the ^{n}Pr-DMQA$^{\bullet}$ neutral radical in acetonitrile and in the presence of aryl halide. (**iv**) Integrated TA signal for ^{n}Pr-DMQA$^{\bullet}$ in the presence of an aryl halide (4-bromo anisole) in acetonitrile at 1:1 ratio and 1:100 ratio for the 520-530 nm region presented on a semi-log scale, (**v**) TA frequency-resolved slices at selected time delays for ^{n}Pr-DMQA$^{\bullet}$ and an aryl halide (4-bromo anisole) at a 1:1 ratio, and (**vi**) a 1:100 ratio. **E.** Proposed con-PET mechanism involving solvated electrons as a key intermediate.

References

1. Prier, C. K., Rankic, D. A. & MacMillan, D. W. C. Visible Light Photoredox Catalysis with Transition Metal Complexes: Applications in Organic Synthesis. *Chemical Reviews* **113**, 5322-5363 (2013).
2. McAtee, R. C., McClain, E. J. & Stephenson, C. R. J. Illuminating Photoredox Catalysis. *Trends in Chemistry* **1**, 111-125 (2019).
3. Romero, N. A. & Nicewicz, D. A. Organic Photoredox Catalysis. *Chemical Reviews* **116**, 10075-10166 (2016).
4. Crisenza, G. E. M. & Melchiorre, P. Chemistry glows green with photoredox catalysis. *Nature Communications* **11**, 803 (2020).
5. Targos, K., Williams, O. P. & Wickens, Z. K. Unveiling Potent Photooxidation Behavior of Catalytic Photoreductants. *Journal of the American Chemical Society* **143**, 4125-4132 (2021).
6. Novaes, L. F. T. *et al.* Electrocatalysis as an enabling technology for organic synthesis. *Chemical Society Reviews* **50**, 7941-8002 (2021).
7. Tay, N. E. S., Lehnherr, D. & Rovis, T. Photons or Electrons? A Critical Comparison of Electrochemistry and Photoredox Catalysis for Organic Synthesis. *Chemical Reviews* **122**, 2487-2649 (2022).
8. Glaser, F., Kerzig, C. & Wenger, O. S. Multi-Photon Excitation in Photoredox Catalysis: Concepts, Applications, Methods. *Angewandte Chemie International Edition* **59**, 10266-10284 (2020).
9. Wu, S., Kaur, J., Karl, T. A., Tian, X. & Barham, J. P. Synthetic Molecular Photoelectrochemistry: New Frontiers in Synthetic Applications, Mechanistic Insights and Scalability. *Angewandte Chemie International Edition* **61**, e202107811 (2022).
10. Liao, L.-L., Song, L., Yan, S.-S., Ye, J.-H. & Yu, D.-G. Highly reductive photocatalytic systems in organic synthesis. *Trends in Chemistry* **4**, 512-527 (2022).
11. Ghosh, I., Ghosh, T., Bardagi, J. I. & König, B. Reduction of aryl halides by consecutive visible light-induced electron transfer processes. *Science* **346**, 725 (2014).
12. Neumeier, M. *et al.* Dichromatic Photocatalytic Substitutions of Aryl Halides with a Small Organic Dye. *Chemistry – A European Journal* **24**, 105-108 (2018).
13. Bardagi, J. I., Ghosh, I., Schmalzbauer, M., Ghosh, T. & König, B. Anthraquinones as Photoredox Catalysts for the Reductive Activation of Aryl Halides. *European Journal of Organic Chemistry* **2018**, 34-40 (2018).
14. Shaikh, R. S., Düsel, S. J. S. & König, B. Visible-Light Photo-Arbuzov Reaction of Aryl Bromides and Trialkyl Phosphites Yielding Aryl Phosphonates. *ACS Catalysis* **6**, 8410-8414 (2016).

15. Cole, J. P. *et al.* Organocatalyzed Birch Reduction Driven by Visible Light. *Journal of the American Chemical Society* **142**, 13573-13581 (2020).
16. Chmiel, A. F., Williams, O. P., Chernowsky, C. P., Yeung, C. S. & Wickens, Z. K. Non-innocent Radical Ion Intermediates in Photoredox Catalysis: Parallel Reduction Modes Enable Coupling of Diverse Aryl Chlorides. *Journal of the American Chemical Society* **143**, 10882-10889 (2021).
17. Xu, J. *et al.* Unveiling Extreme Photoreduction Potentials of Donor–Acceptor Cyanoarenes to Access Aryl Radicals from Aryl Chlorides. *Journal of the American Chemical Society* **143**, 13266-13273 (2021).
18. MacKenzie, I. A. *et al.* Discovery and characterization of an acridine radical photoreductant. *Nature* **580**, 76-80 (2020).
19. Graml, A., Neveselý, T., Jan Kutta, R., Cibulka, R. & König, B. Deazaflavin reductive photocatalysis involves excited semiquinone radicals. *Nature Communications* **11**, 3174 (2020).
20. Rieth, A. J., Gonzalez, M. I., Kudisch, B., Nava, M. & Nocera, D. G. How Radical Are "Radical" Photocatalysts? A Closed-Shell Meisenheimer Complex Is Identified as a Super-Reducing Photoreagent. *Journal of the American Chemical Society* **143**, 14352-14359 (2021).
21. Herse, C. *et al.* A Highly Configurationally Stable [4]Heterohelicenium Cation. *Angewandte Chemie International Edition* **42**, 3162-3166 (2003).
22. Laursen, B. W. & Krebs, F. C. Synthesis of a Triazatriangulenium Salt. *Angewandte Chemie International Edition* **39**, 3432-3434 (2000).
23. Mei, L., Veleta, J. M. & Gianetti, T. L. Helical Carbenium Ion: A Versatile Organic Photoredox Catalyst for Red-Light-Mediated Reactions. *Journal of the American Chemical Society* **142**, 12056-12061 (2020).
24. Mei, L., Moutet, J., Stull, S. M. & Gianetti, T. L. Synthesis of CF3-Containing Spirocyclic Indolines via a Red-Light-Mediated Trifluoromethylation/Dearomatization Cascade. *The Journal of Organic Chemistry* **86**, 10640-10653 (2021).
25. Shaikh, A. C. *et al.* Persistent, highly localized, and tunable [4]helicene radicals. *Chemical Science* **11**, 11060-11067 (2020).
26. Sørensen, T. J., Nielsen, M. F. & Laursen, B. W. Synthesis and Stability of N,N′-Dialkyl-1,13-dimethoxyquinacridinium (DMQA+): A [4]Helicene with Multiple Redox States. *ChemPlusChem* **79**, 1030-1035 (2014).
27. Kerzig, C., Guo, X. & Wenger, O. S. Unexpected Hydrated Electron Source for Preparative Visible-Light Driven Photoredox Catalysis. *Journal of the American Chemical Society* **141**, 2122-2127 (2019).

28. Naumann, R., Lehmann, F. & Goez, M. Generating Hydrated Electrons for Chemical Syntheses by Using a Green Light-Emitting Diode (LED). *Angewandte Chemie International Edition* **57**, 1078-1081 (2018).
29. Enemærke, R. J., Christensen, T. B., Jensen, H. & Daasbjerg, K. Application of a new kinetic method in the investigation of cleavage reactions of haloaromatic radical anions. *Journal of the Chemical Society, Perkin Transactions 2*, 1620-1630 (2001).
30. Constantin, T., Juliá, F., Sheikh, N. S. & Leonori, D. A case of chain propagation: α-aminoalkyl radicals as initiators for aryl radical chemistry. *Chemical Science* **11**, 12822-12828 (2020).
31. Hossain, M. M., Shaikh, A. C., Moutet, J. & Gianetti, T. L. Photocatalytic α-arylation of cyclic ketones. *Nature Synthesis* **1**, 147-157 (2022).
32. Ban, H. S. & Nakamura, H. Boron-Based Drug Design. *The Chemical Record* **15**, 616-635 (2015).
33. Conreaux, D., Mehanna, N., Herse, C. & Lacour, J. From Cationic to Anionic Helicenes: New Reactivity through Umpolung. *The Journal of Organic Chemistry* **76**, 2716-2722 (2011).
34. Bosson, J., Labrador, G. M., Besnard, C., Jacquemin, D. & Lacour, J. Chiral Near-Infrared Fluorophores by Self-Promoted Oxidative Coupling of Cationic Helicenes with Amines/Enamines. *Angewandte Chemie International Edition* **60**, 8733-8738 (2021).
35. Fujitsuka, M. & Majima, T. Reaction dynamics of excited radical ions revealed by femtosecond laser flash photolysis. *Journal of Photochemistry and Photobiology C: Photochemistry Reviews* **35**, 25-37 (2018).
36. Gosztola, D., Niemczyk, M. P., Svec, W., Lukas, A. S. & Wasielewski, M. R. Excited Doublet States of Electrochemically Generated Aromatic Imide and Diimide Radical Anions. *The Journal of Physical Chemistry A* **104**, 6545-6551 (2000).
37. Bonin, M. A., Tsuji, K. & Williams, F. Electron Spin Resonance Evidence for a Trapped Electron and its Reversible Reaction in Gamma-irradiated Acetonitrile-d3. *Nature* **218**, 946-948 (1968).
38. Ayscough, P. B., Collins, R. G. & Kemp, T. J. Electron Spin Resonance Studies of Fundamental Processes in Radiation and Photochemistry. II. Photochemical Reactions in γ-Irradiated Nitriles at 77°K. *The Journal of Physical Chemistry* **70**, 2220-2223 (1966).
39. Fleischmann, M., Mengoli, G. & Pletcher, D. The cathodic reduction of acetonitrile: A new synthesis of tin tetramethyl. *Journal of Electroanalytical Chemistry and Interfacial Electrochemistry* **43**, 308-310 (1973).
40. Grills, D. C. & Lymar, S. V. Solvated Electron in Acetonitrile: Radiation Yield, Absorption Spectrum, and Equilibrium between Cavity- and Solvent-Localized States. *The Journal of Physical Chemistry B* **126**, 262-269 (2022).

41. Doan, S. C. & Schwartz, B. J. Ultrafast Studies of Excess Electrons in Liquid Acetonitrile: Revisiting the Solvated Electron/Solvent Dimer Anion Equilibrium. *The Journal of Physical Chemistry B* **117**, 4216-4221 (2013).
42. Mortensen, J. & Heinze, J. The Electrochemical Reduction of Benzene—First Direct Determination of the Reduction Potential. *Angewandte Chemie International Edition in English* **23**, 84-85 (1984).